Original Article | Open Access

Journal of Cancer Metastasis and Treatment

Shen *et al. J Cancer Metastasis Treat.* 2026;12:6 **DOI:**10.20517/2394-4722.2026.07

Integrated transcriptomics identifies *ITGB5* as a hub linking coding and non-coding RNAs to signaling regulation in hepatocellular carcinoma

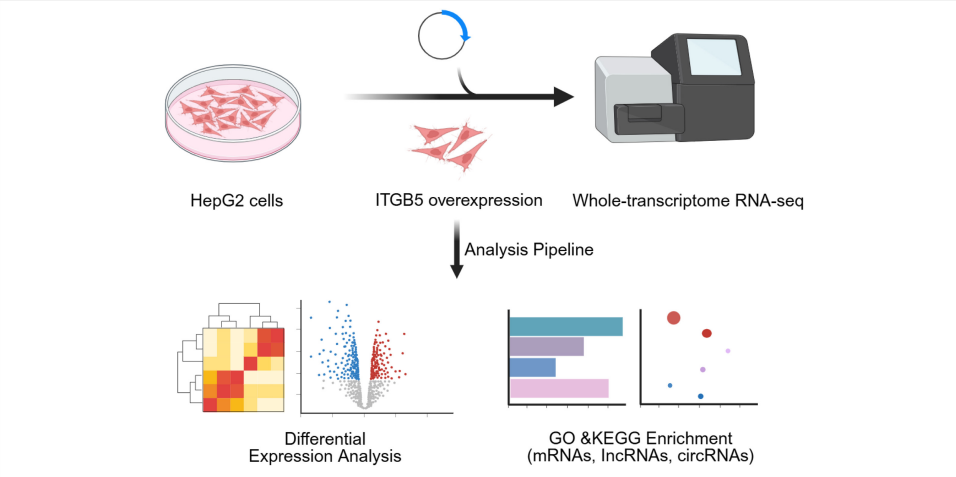
Wenke Shen[1,#], Jingru Wang[1,#], Qihang Zeng[1,#], Guiqiang Li[1], Qi Xin[1], Zepeng Lin[1], Delong Yang[1], Xiaodong Chen[1], Jia He[1,2]

Keywords:
ITGB5, hepatocellular carcinoma, transcriptome profiling, PI3K/Akt pathway, MAPK/ERK pathway

Citation: Shen W, Wang J, Zeng Q, Li G, Xin Q, Lin Z, Yang D, Chen X, He J. Integrated transcriptomics identifies *ITGB5* as a hub linking coding and non-coding RNAs to signaling regulation in hepatocellular carcinoma. *J Cancer Metastasis Treat.* 2026;12:6. https://dx.doi.org/10.20517/2394-4722.2026.07

Received: 2 Feb 2026
First Decision: 27 Mar 2026
Revised: 9 Apr 2026
Accepted: 23 Apr 2026
Published: 30 Apr 2026

Academic Editor: Hailin Tang
Copy Editor: Ping Zhang
Production Editor: Ping Zhang



Abstract

Aim: To elucidate integrin β5 (*ITGB5*)-associated transcriptomic alterations in hepatocellular carcinoma cells and identify key coding and non-coding RNA regulators and their associated signaling pathways.

Methods: Whole-transcriptome sequencing was conducted on HepG2 (human hepatocellular carcinoma cell line) cells overexpressing *ITGB5*. Differential expression analysis was performed, followed by Gene Ontology (GO) and Kyoto Encyclopedia of Genes and Genomes (KEGG) enrichment analyses for messenger RNAs (mRNAs), long non-coding RNAs (lncRNAs), and circular RNAs (circRNAs). Candidate transcripts were validated using real-time quantitative polymerase chain reaction (RT-qPCR).

Results: *ITGB5* overexpression induced extensive transcriptomic alterations. KEGG

[1]Department of Burn Surgery, The First People's Hospital of Foshan (Foshan Hospital Affiliated to Southern University of Science and Technology), Foshan 528000, Guangdong, China.
[2]Institute of Translational Medicine, The First People's Hospital of Foshan (Foshan Hospital Affiliated to Southern University of Science and Technology), Foshan 528000, Guangdong, China.
[#]The authors contributed equally to this work.

Correspondence to: Dr. Delong Yang, Dr. Xiaodong Chen, Department of Burn Surgery, The First People's Hospital of Foshan (Foshan Hospital Affiliated to Southern University of Science and Technology), Foshan 528000, Guangdong, China. E-mail: dlyangxmu@outlook.com; cxd234@163.com; Dr. Jia He, Department of Burn Surgery, The First People's Hospital of Foshan (Foshan Hospital Affiliated to Southern University of Science and Technology), Foshan 528000, Guangdong, China; Institute of Translational Medicine, The First People's Hospital of Foshan (Foshan Hospital Affiliated to Southern University of Science and Technology), Foshan

528000, Guangdong, China. E-mail: hejia021@126.com

enrichment highlighted the phospholipase D, vascular endothelial growth factor (VEGF), and ErbB signaling pathways, with significant involvement of the phosphoinositide 3-kinase/protein kinase B (PI3K/Akt) and mitogen-activated protein kinase/extracellular signal-regulated kinase (MAPK/ERK) cascades. Pathway-level analyses suggested a relative attenuation of PI3K/Akt signaling alongside the preferential engagement of MAPK/ERK-related programs. GO analysis indicated shifts in biological processes, notably the negative regulation of peptidase activity and cell-matrix adhesion. Furthermore, *ITGB5* was associated with widespread lncRNA and circRNA regulation; predicted target genes of these non-coding RNAs were enriched in PI3K/Akt signaling, protein processing in the endoplasmic reticulum, and cell cycle regulation. RT-qPCR confirmed the upregulation of key transcripts, including dystroglycan 1 (*DAG1*; mRNA), small nucleolar RNA host gene 1 (*SNHG1*; lncRNA), and *circFN1* (circRNA), in *ITGB5*-overexpressing cells.

Conclusion: Our findings identify *ITGB5* as a regulatory hub in hepatocellular carcinoma (HCC) associated with coding and non-coding RNA regulatory networks, offering insights into potential therapeutic targets.

INTRODUCTION

Hepatocellular carcinoma (HCC) remains one of the most prevalent and lethal malignancies worldwide[1,2]. Despite advances in targeted therapies and immunotherapy, the prognosis for patients with advanced HCC remains poor due to high rates of drug resistance, metastasis, and recurrence[3-5]. These challenges underscore the urgent need to identify novel molecular regulators and signaling networks that drive hepatocarcinogenesis and may serve as biomarkers or therapeutic targets.

Integrins play pivotal roles in essential cellular processes - including adhesion, migration, proliferation, and survival - primarily by mediating interactions between cells and the extracellular matrix (ECM) and activating downstream signaling[6]. Aberrant integrin signaling is frequently implicated in tumor invasion, metastatic dissemination, and therapy resistance[7-9]. Among these, integrin β5 (*ITGB5*) has been shown to promote malignant phenotypes by activating the Wnt/β-catenin (Wingless/Integrated and β-catenin) signaling pathway, transforming growth factor β (TGF-β), and phosphoinositide 3-kinase/protein kinase B (PI3K/Akt) pathways[9,10]. In HCC, elevated *ITGB5* expression correlates with aggressive clinicopathological features and poor prognosis[11,12]. However, most studies have focused on protein-level alterations or specific signaling pathways. As a result, the comprehensive transcriptomic programs regulated by *ITGB5* in HCC remain largely undefined[7,13].

In the era of precision oncology, integrated transcriptomic analyses incorporating both coding and non-coding RNA layers are essential for elucidating complex regulatory networks. Non-coding RNAs, particularly long non-coding RNAs (lncRNAs) and circular RNAs (circRNAs), have emerged as critical regulators of gene expression in cancer. lncRNAs can influence chromatin dynamics and transcription, while circRNAs frequently function as competing endogenous RNAs (ceRNAs) to modulate target messenger RNA (mRNA) stability[14,15]. Although dysregulation of these non-coding RNAs has been linked to oncogenic pathways in HCC, how *ITGB5* integrates these layers into coherent regulatory networks remains poorly understood.

To address these gaps, we performed whole-transcriptome sequencing to compare *ITGB5*-overexpressing and control HepG2 (human hepatocellular carcinoma cell line) cells. We characterized *ITGB5*-dependent transcriptomic reprogramming, identified differentially expressed RNAs, and mapped their functional

enrichment using Gene Ontology (GO) and Kyoto Encyclopedia of Genes and Genomes (KEGG) pathway analyses. Furthermore, we identified dystroglycan 1 (DAG1), small nucleolar RNA host gene 1 (SNHG1), and *circFN1* as significant candidates within this network. This work defines a multilayered *ITGB5*-regulated transcriptomic architecture in HCC and provides a robust framework for future mechanistic investigations into how *ITGB5* reshapes oncogenic signaling.

MATERIALS AND METHODS

Cell culture

HepG2 cells were cultured in RPMI-1640 medium (Wisent, Canada) supplemented with 10% fetal bovine serum (FBS; Wisent, China) and 1% penicillin-streptomycin (P/S; Gibco, USA). HEK293T (human embryonic kidney 293T) cells were maintained in high-glucose Dulbecco's modified Eagle medium (DMEM; Gibco, USA) containing 10% FBS and 1% P/S. Both cell lines were obtained from the Cell Bank of the Type Culture Collection of the Chinese Academy of Sciences (Shanghai, China) and maintained in a humidified incubator at 37 °C with 5% CO_2.

Construction of *ITGB5* overexpression lentivirus and cell transduction

The coding DNA sequence (CDS) of human *ITGB5* [National Center for Biotechnology Information (NCBI) Reference Sequence: NM_002213.5] was amplified from human fibroblast complementary DNA (cDNA) using Q5 High-Fidelity DNA Polymerase (New England Biolabs, USA). The polymerase chain reaction (PCR)-amplified fragment was cloned into the pLV-mCherry vector (Addgene plasmid #36084) via *Bsr*GI and *Sal*I restriction sites. The resulting pLV-mCherry-*ITGB5* construct was validated by Sanger sequencing. Lentiviral particles were produced by co-transfecting HEK293T cells with either the pLV-mCherry-*ITGB5* or the pLV-mCherry (control) plasmid, along with the packaging vectors HIV-1 Rev expression plasmid (pREV), HIV-1 gag/pol packaging plasmid (pMDL), and vesicular stomatitis virus glycoprotein expression plasmid (pVSVG), using PolyJet transfection reagent (SignaGen Laboratories, USA) according to the manufacturer's instructions. Viral supernatants were harvested 48 h post-transfection, passed through a 0.45-μm filter, and stored at -80 °C until use.

HepG2 cells were seeded and cultured to approximately 70% confluence prior to infection. The cells were then transduced with LV-mCherry-*ITGB5* or control lentiviral particles in the presence of 5 μg/mL polybrene (Sigma-Aldrich, USA). After a 12 h incubation, the viral suspension was replaced with fresh complete medium, and the cells were maintained for 10 days to establish stable overexpression. *ITGB5*-overexpressing cells were subsequently harvested for downstream analyses, including RNA extraction and whole-transcriptome sequencing.

RNA extraction and RT-qPCR

Total RNA was extracted from *ITGB5*-overexpressing and control HepG2 cells using a total RNA extraction kit (Omega, USA) according to the manufacturer's instructions. cDNA synthesis was performed using the PrimeScript™ RT Reagent Kit with gDNA Eraser (Takara, Japan). Real-time quantitative PCR (RT-qPCR) was conducted using the SYBR Premix Ex Taq II (Takara). Primers were specifically designed to span exon-exon junctions for linear transcripts or back-splice junctions for circRNAs. The primer sequences used in this study were as follows: *ITGB5* Forward: 5'-GTCTGCTAATCCACCCAAAATG-3', Reverse: 5'-TCTCTATCTCACCTCCACAGC-3'; *DAG1* Forward: 5'-CCACAGTGGTTGGCATTCCTGA-3', Reverse: 5'-CCAAGATGGCAAAGCCTCCTTC-3'; *SNHG1* Forward: 5'-CTGTTCCCGTCATGAGCCTT-3', Reverse: 5'-GCAAGGCCCTGAATGAGCTA-3'; *circFN1* Forward: 5'-GGAGAAGTATGTGCATGGTGTCA-3', Reverse: 5'-TGCAGATTTCCTCGTGGGTTG-3'; and *GAPDH* Forward: 5'-TGCACCACCAACTGCTTAGC-3', Reverse: 5'-GGCATGGACTGTGGTCATGAG-3'. GAPDH was used as the internal normalization control.

Thermal cycling conditions consisted of an initial denaturation at 95 °C for 30 s, followed by 40 cycles of denaturation at 95 °C for 5 s and annealing/extension at 60 °C for 10 s. Relative gene expression levels were calculated using the $2^{-\Delta\Delta Ct}$ method. All reactions were performed in triplicate, and each experiment was independently repeated at least three times.

Library preparation and RNA sequencing

Sequencing libraries were constructed using two complementary strategies to profile both coding and non-coding transcriptomes. For mRNA sequencing, 1 μg of total RNA per sample was used to generate libraries with the NEBNext® Ultra™ RNA Library Prep Kit for Illumina®. Briefly, poly(A)$^+$ mRNA was enriched using oligo(dT)25 magnetic beads and fragmented. Double-stranded cDNA was synthesized, ligated to single-index adapters, and PCR-amplified.

To comprehensively characterize non-coding RNAs, including lncRNAs, strand-specific libraries were prepared. Ribosomal RNA (rRNA) was depleted using a rRNA Removal Kit, and the remaining RNA was fragmented. Strand-specific cDNA libraries were constructed using a deoxyuridine triphosphate (dUTP)-based second-strand marking strategy, followed by uracil-N-glycosylase digestion to preserve strand orientation. All libraries were assessed for quality using an Agilent Bioanalyzer 2100. Libraries with concentrations > 2 nM were pooled and sequenced on the Illumina NovaSeq™ 6000 platform to generate 150-bp paired-end reads.

Sequence data processing and analysis

Sequence data processing

Raw sequencing reads in FASTQ format were processed with fastp to remove adapter sequences, poly-N reads, and low-quality bases. All libraries exhibited high quality, with Q30 values ranging from 95.79% to 96.74% [Supplementary Table 1]. The resulting clean reads were aligned to the human reference genome (GRCh38) using HISAT2 (v2.0.5), with splice-aware mapping enabled using gene annotation. Transcripts were subsequently assembled using StringTie and merged across samples with gffcompare to generate a unified transcriptome. Gene expression levels were quantified using RNA-Seq by Expectation Maximization (RSEM); specifically, expected read counts were utilized for differential expression analysis, whereas fragments per kilobase of transcript per million mapped reads (FPKM) values were used for expression visualization. Three biological replicates were included for each group.

Differential expression analysis

Differential expression analysis was performed using the DESeq2 R package, which utilizes a negative binomial distribution model to analyze digital gene expression data. To control the false discovery rate (FDR), *P* values were adjusted for multiple testing using the Benjamini-Hochberg method. Genes meeting the criteria of |log2 fold change| ≥ 2 and an adjusted *P* value (padj) < 0.05 were considered significantly differentially expressed.

Enrichment analysis of differentially expressed genes

Functional enrichment analyses, including GO and KEGG analyses, were conducted using the clusterProfiler R package to evaluate the statistical enrichment of differentially expressed genes (DEGs). To ensure accuracy, gene length bias was corrected during GO enrichment analysis. Terms and pathways with an adjusted $P < 0.05$ were considered significantly enriched.

Gene set enrichment analysis

Gene set enrichment analysis (GSEA) was performed to determine whether predefined gene sets showed coordinated differences between the two groups, independent of an explicit DEG cutoff. Briefly, all genes were ranked according to their log2 fold change between the two groups, and predefined gene sets were tested to determine whether their member genes were preferentially enriched at the top or bottom of the ranked list. Gene sets from the GO, KEGG, and Molecular Signatures Database (MSigDB) collections (including Reactome) were analyzed independently. Enrichment significance was assessed using the FDR-adjusted *P* values, and gene sets with an FDR < 0.05 were considered significantly enriched.

Network analysis

Network analysis was conducted based on significantly enriched KEGG pathways and predicted regulatory relationships. DEGs associated with significantly enriched KEGG pathways were mapped onto KEGG pathway diagrams, and pathway interaction networks were constructed and visualized using Cytoscape. In the pathway network, nodes represent genes or pathways, while edges represent pathway-associated relationships derived from KEGG pathway annotations. For lncRNA-related network analysis, cis- and trans-regulatory networks were generated based on predicted target relationships. Protein-coding genes located within 100 kb upstream or downstream of a given lncRNA were defined as potential cis-target genes[16], while potential trans-target genes were inferred via Pearson correlation analysis between lncRNAs and coding genes[17]. In these networks, nodes represent lncRNAs or target genes, and edges represent predicted regulatory associations. For circRNA-related network analysis, potential microRNA (miRNA) binding sites on differentially expressed circRNAs were predicted using miRanda and TargetScan. Candidate circRNA-miRNA pairs were retained only when they were supported by both tools and satisfied the following thresholds: miRanda score > 140 and free energy < -20 kcal/mol. A circRNA-miRNA interaction network was subsequently constructed based on these associations. In this network, nodes represent circRNAs or miRNAs, and edges represent predicted interaction relationships.

Statistical analysis

All statistical plots were generated using GraphPad Prism 10.0 (GraphPad Software, San Diego, CA, USA). A two-tailed unpaired Student's *t*-test was employed for comparisons between two groups. Statistical significance was defined as follows: $^{*}P < 0.05$, $^{**}P < 0.01$, $^{***}P < 0.001$, and $^{****}P < 0.0001$.

RESULTS

Establishment of the *ITGB5* overexpression model and global transcriptomic analysis

To investigate the global regulatory roles of *ITGB5*, we established a stable *ITGB5*-overexpressing HepG2 cell line using a lentiviral transduction system. RT-qPCR analysis confirmed a marked increase in *ITGB5* mRNA levels in the overexpression group compared with the empty vector control [Supplementary Figure 1].

Transcriptome-wide profiling reveals extensive gene and transcript alterations induced by *ITGB5* overexpression

To characterize the transcriptomic impact of *ITGB5* overexpression, whole-transcriptome sequencing was performed on *ITGB5*-OE (*ITGB5* overexpression) and control cells. Principal component analysis (PCA) demonstrated a clear separation between the *ITGB5*-OE and control groups, with biological replicates clustering tightly within each group. These findings confirmed the high reproducibility of our data and the distinct transcriptional profiles induced by *ITGB5* overexpression [Figure 1A and B].

DESeq2 analysis identified 95 DEGs (54 upregulated and 41 downregulated) and 2,032 differentially expressed transcripts (DETs; 1,022 upregulated and 1,010 downregulated) [Figure 1C and D, Figure 2A, Supplementary Table 2]. Heatmap visualization further confirmed that these DEGs and DETs were robustly

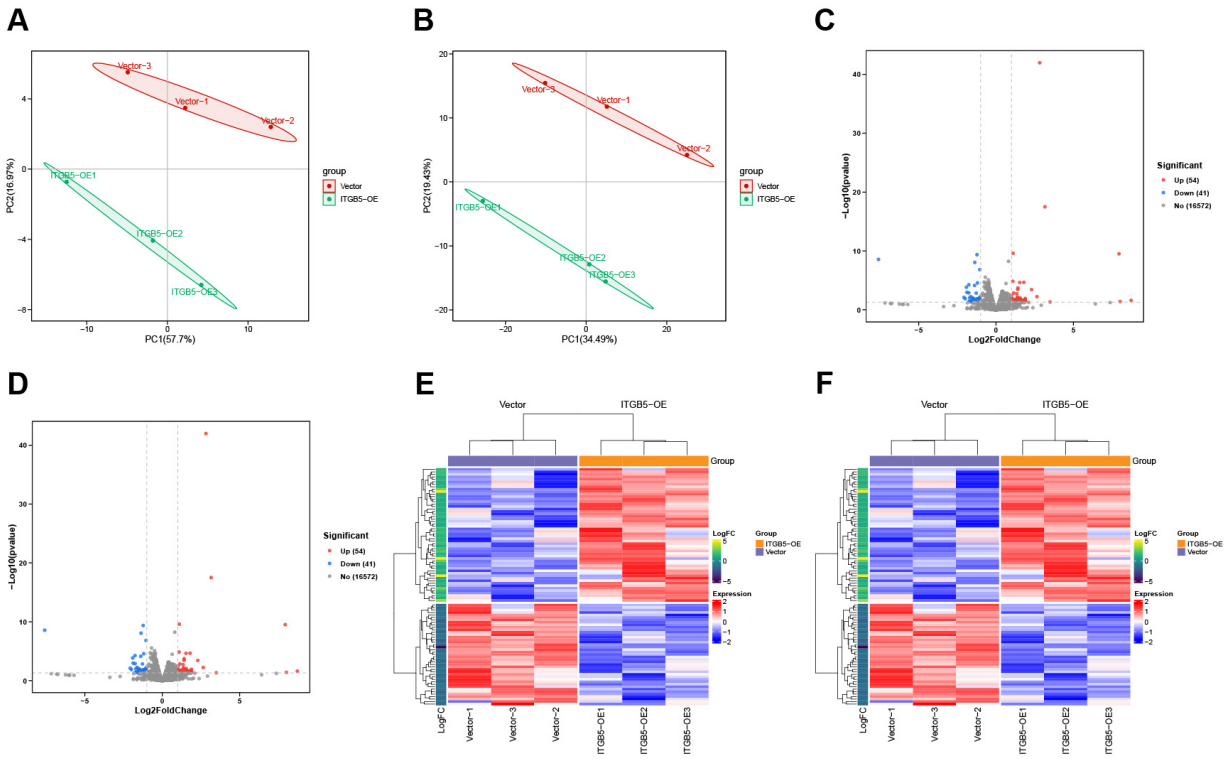


Figure 1. Transcriptomic landscapes and differential expression profiles following *ITGB5* overexpression. (A) Principal component analysis (PCA) plot based on differentially expressed genes (DEGs); (B) PCA plot based on differentially expressed transcripts (DETs); (C) Volcano plot depicting DEGs; (D) Volcano plot depicting DETs; (E) Heatmap illustrating the expression of DEGs; (F) Heatmap illustrating the expression of DETs.

regulated by *ITGB5* across all biological replicates [Figure 1E and F].

ITGB5 broadly activates oncogenic signaling pathways and modulates key cellular functions

To examine the biological implications of *ITGB5*-driven transcriptional changes, we conducted GO and KEGG enrichment analyses on the identified DEGs. Overall, *ITGB5* overexpression was predominantly associated with pathways related to cell adhesion, oncogenic signaling, and intracellular regulatory processes.

At the gene level, GO enrichment analysis highlighted biological programs linked to cell-matrix adhesion and the regulation of proteolysis [Figure 2B and Supplementary Table 3]. Concurrently, KEGG analysis indicated that the DEGs were primarily enriched in pathways converging on the PI3K/Akt and mitogen-activated protein kinase/extracellular signal-regulated kinase (MAPK/ERK) signaling axes, including phospholipase D, vascular endothelial growth factor (VEGF), and ErbB signaling [Figure 2C and Supplementary Table 4].

At the transcript level, GO enrichment of DETs revealed processes associated with cell architecture and epigenetic regulation, including focal adhesion, chromatin remodeling, and serine/threonine kinase activity [Figure 2D and Supplementary Table 5]. KEGG analysis of these DETs further indicated enrichment in pathways related to viral infections (including hepatitis B and C), cellular senescence, and FoxO signaling [Figure 2E and Supplementary Table 6].

Convergence of complex signaling networks on PI3K/Akt and MAPK/ERK pathways

To further characterize the signaling architecture downstream of *ITGB5*, we performed complementary GSEA and network analyses. GSEA using GO and MSigDB/Reactome gene sets revealed a clear separation between suppressed and activated biological programs [Supplementary Figure 2A and B].

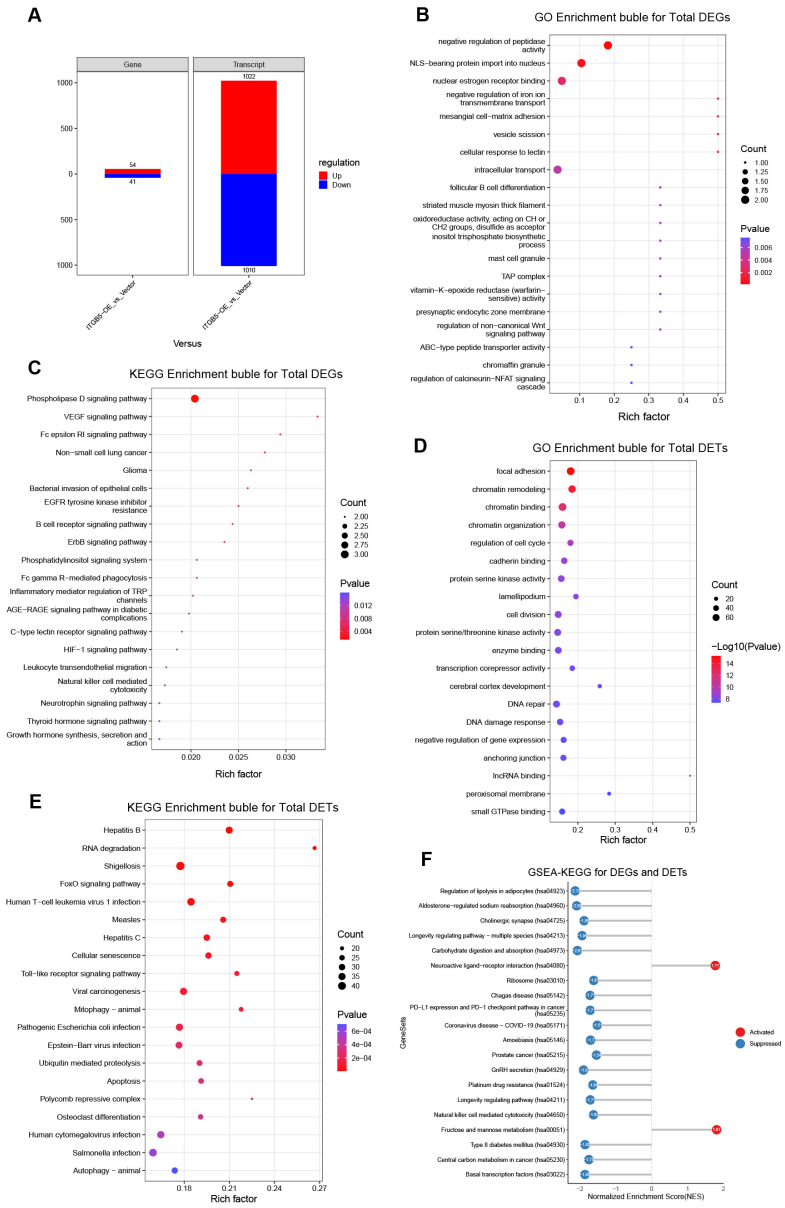


Figure 2. Functional enrichment landscapes of DEGs and DETs following *ITGB5* overexpression. (A) Summary of up- and downregulated genes and transcripts; (B) Gene Ontology (GO) enrichment bubble plot for all DEGs; (C) Kyoto Encyclopedia of Genes and Genomes (KEGG) enrichment bubble plot for all DEGs; (D) GO enrichment bubble plot for all DETs; (E) KEGG enrichment bubble plot for all DETs; (F) Gene set enrichment analysis based on KEGG pathways (GSEA-KEGG) for integrated DEGs and DETs (activated pathways in red; suppressed pathways in blue). DEGs: Differentially expressed genes; DETs: differentially expressed transcripts; VEGF: vascular endothelial growth factor; TAP: transporter associated with antigen processing; NFAT: nuclear factor of activated T cells; NLS: nuclear localization signal; IRF: interferon regulatory factor; EGFR: epidermal growth factor receptor; TRP: transient receptor potential; AGE-RAGE: advanced glycation end products-receptor for advanced glycation end products; HIF-1: hypoxia-inducible factor 1; lncRNA: long non-coding RNA.

Specifically, suppressed signatures were dominated by RNA processing/splicing and translation-related modules, alongside attenuated mitochondrial respiration and oxidative phosphorylation (OXPHOS) pathways. In contrast, activated signatures encompassed G protein-coupled receptor (GPCR)-related signaling, transmembrane transport, carbohydrate metabolism/gluconeogenesis, and sulfation/sulfotransferase-associated processes.

Network analysis of significantly enriched KEGG pathways highlighted PI3K/Akt and MAPK/ERK as major convergent nodes, supporting their roles as core regulatory axes in the *ITGB5* downstream network [Supplementary Figure 2C]. Furthermore, KEGG-GSEA confirmed the perturbation of these two cascades

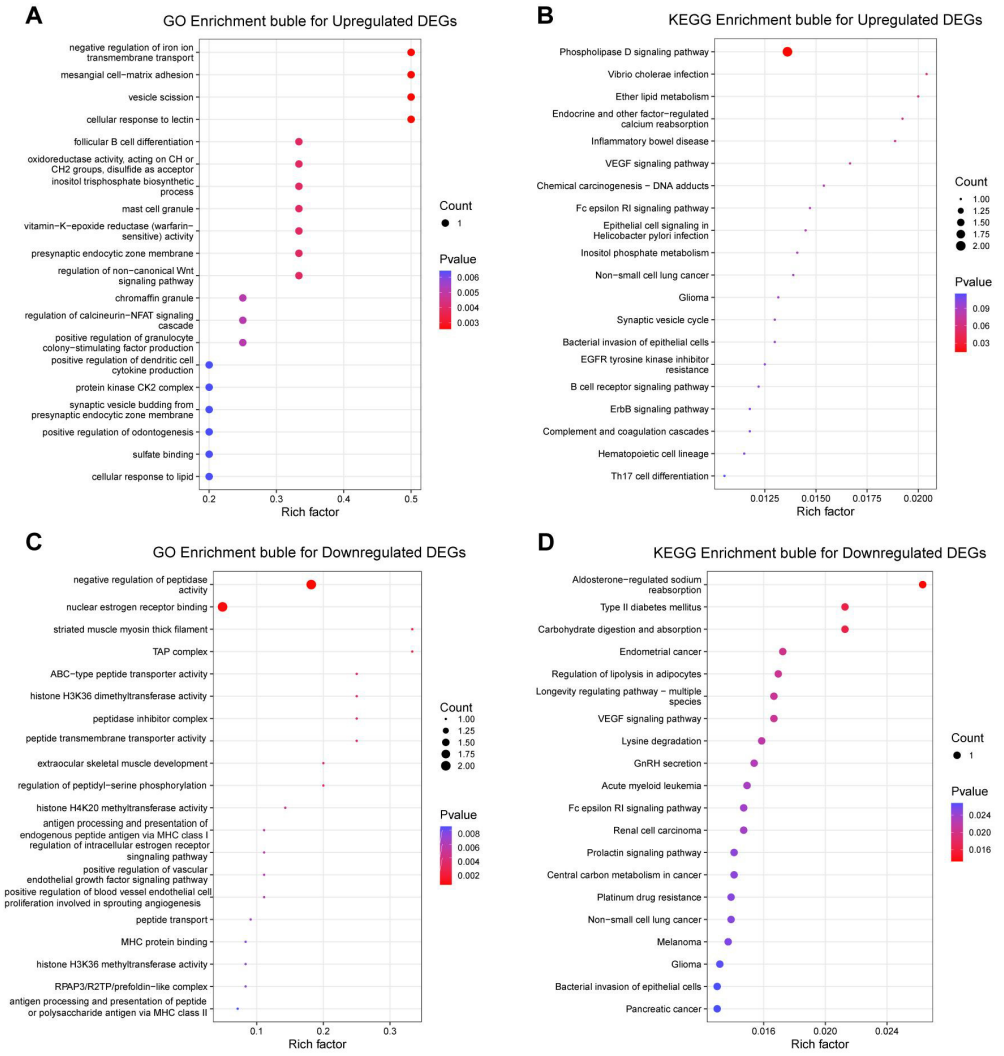


Figure 3. GO and KEGG enrichment analyses of upregulated and downregulated DEGs following *ITGB5* overexpression. (A) GO enrichment bubble plot for upregulated DEGs; (B) KEGG enrichment bubble plot for upregulated DEGs; (C) GO enrichment bubble plot for downregulated DEGs; (D) KEGG enrichment bubble plot for downregulated DEGs. DEGs: Differentially expressed genes; DETs: differentially expressed transcripts; GO: gene ontology; KEGG: kyoto encyclopedia of genes and genomes; VEGF: vascular endothelial growth factor; EGFR: epidermal growth factor receptor; TAP: transporter associated with antigen processing; ABC: ATP-binding cassette; MHC: major histocompatibility complex; NFAT: nuclear factor of activated T cells.

across multiple enriched pathways, including the cholinergic synapse, longevity-regulating pathways, carbohydrate digestion and absorption, the programmed death ligand 1/programmed cell death protein 1 (PD-L1/PD-1) checkpoint, prostate cancer, gonadotropin-releasing hormone (GnRH) secretion, platinum drug resistance, natural killer (NK) cell-mediated cytotoxicity, and central carbon metabolism in cancer [Figure 2F].

Functional enrichment of up- and downregulated DEGs

Differential expression analysis further revealed distinct functional signatures between upregulated and downregulated DEGs. Specifically, upregulated genes were primarily enriched in signaling and membrane-trafficking programs associated with the phospholipase D, VEGF, and ErbB-related pathways, consistent with the activation of *ITGB5*-linked oncogenic signaling [Figure 3A and B]. In contrast, downregulated genes were predominantly associated with antigen presentation, peptidase regulation, and selected metabolic or endocrine-related pathways [Figure 3C and D]. Collectively, these findings suggest that *ITGB5* overexpression preferentially amplifies signaling programs governing cell communication and tumor progression while suppressing a subset of homeostatic and regulatory processes.

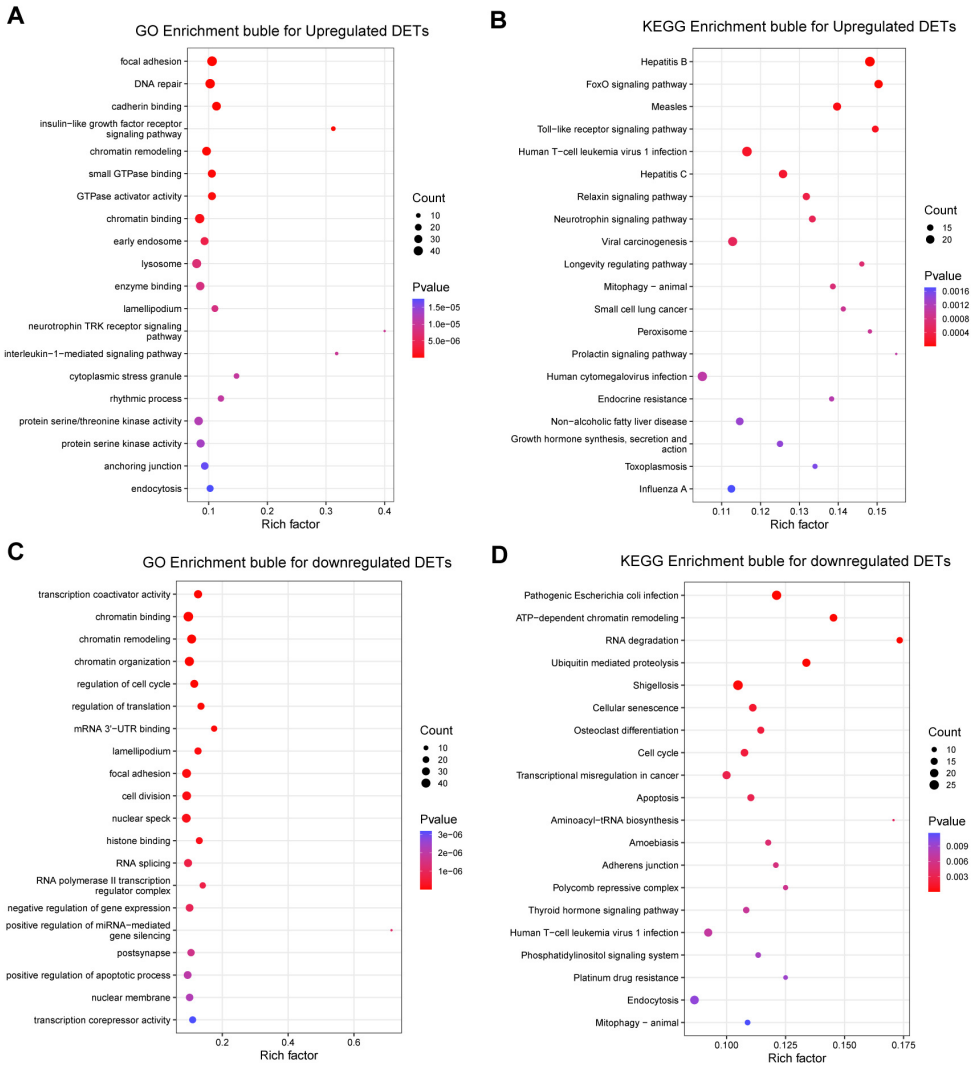


Figure 4. GO and KEGG enrichment profiles of upregulated and downregulated DETs following *ITGB5* overexpression. (A) GO enrichment bubble plot illustrating upregulated DETs; (B) KEGG enrichment bubble plot illustrating upregulated DETs; (C) GO enrichment bubble plot illustrating downregulated DETs; (D) KEGG enrichment bubble plot illustrating downregulated DETs. DEGs: Differentially expressed genes; DETs: differentially expressed transcripts; GO: gene ontology; KEGG: kyoto encyclopedia of genes and genomes; TRK: tropomyosin receptor kinase; 3′UTR: 3′ untranslated region; ATP: adenosine triphosphate.

Functional enrichment of up- and downregulated DETs

GO and KEGG analyses of DETs demonstrated that *ITGB5*-induced transcript-level alterations were primarily linked to cell-matrix interaction, intracellular trafficking, chromatin regulation, and RNA processing. Upregulated transcripts were enriched in focal adhesion- and signaling-related processes [Figure 4A and B], whereas downregulated transcripts were more closely associated with transcriptional regulation, chromatin remodeling, RNA metabolism, and cell-cycle control [Figure 4C and D].

ITGB5 regulates a non-coding RNA network associated with stress response and signal transduction

To further elucidate the regulatory effects of *ITGB5* beyond protein-coding genes, we examined its impact on non-coding RNAs. At the transcript level, we identified 89,832 mRNAs alongside 223,395 annotated lncRNA transcripts and 1,142 novel lncRNA candidates [Supplementary Figure 3A], which were broadly distributed across the genome [Supplementary Figure 3B]. Differential analysis revealed 385 lncRNA transcripts significantly altered by *ITGB5* overexpression (174 upregulated and 211 downregulated), as illustrated by

volcano plot and hierarchical clustering analyses [Supplementary Figure 3C and D, Supplementary Table 7]. When summarized at the gene level, 39 non-coding RNA loci were differentially expressed (17 upregulated and 22 downregulated), and these changes similarly distinguished *ITGB5*-OE from vector controls [Supplementary Figure 3E and F, Supplementary Table 8].

To explore the functional implications of *ITGB5*-regulated lncRNAs, we predicted their *cis*- and *trans*-target genes and visualized the corresponding regulatory networks [Figure 5A and B, Supplementary Table 9]. GO enrichment of *cis*-target genes indicated associations with cellular responses to hypoxia, RNA splicing/mRNA degradation, protein quality control, and integrin-mediated signaling [Figure 5C]. Concurrently, KEGG analysis highlighted significant enrichment in the PI3K/Akt signaling pathway and protein processing in the endoplasmic reticulum [Figure 5D]. In parallel, GO enrichment of *trans*-target genes was dominated by chromatin remodeling, endoplasmic reticulum stress, RNA splicing, and the regulation of apoptosis [Figure 5E], while KEGG analysis further supported enrichment in RNA splicing-related pathways and the endoplasmic reticulum unfolded protein response (UPR) [Figure 5F].

Consistent with these transcriptome-wide changes, circRNA profiling indicated that *ITGB5* overexpression modulated the circRNA landscape without markedly altering global size characteristics, as circRNA length distributions were highly similar between groups [Figure 6A]. Sample-wise expression patterns further confirmed robust circRNA detection across replicates [Figure 6B]. Differential analysis identified 251 dysregulated circRNAs (120 upregulated and 131 downregulated) in *ITGB5*-OE versus vector controls [Figure 6C and Supplementary Table 10]. Heatmap visualization coupled with unsupervised hierarchical clustering clearly distinguished *ITGB5*-OE samples from controls [Figure 6D], indicating a distinct *ITGB5*-associated circRNA signature.

To infer potential functions, we analyzed the host genes of the dysregulated circRNAs. GO enrichment was dominated by genome integrity and mitotic regulation, including the DNA damage response/repair, microtubule-kinetochore organization, and cell division-related processes [Figure 6E]. KEGG analysis reinforced these themes, highlighting DNA replication, the cell cycle, homologous recombination, and ubiquitin-mediated proteolysis, as well as nucleocytoplasmic transport and MAPK signaling [Figure 6F]. In parallel, the predicted circRNA-miRNA interaction network suggested extensive regulatory connectivity [Figure 6G], consistent with a potential post-transcriptional modulatory role for *ITGB5*-responsive circRNAs. Finally, coding-potential assessment showed minimal overlap among predictions from Coding-Non-Coding Index (CNCI), Coding Potential Calculator 2 (CPC2), Pfam, and internal ribosome entry site (IRES) [Figure 6H], supporting the conclusion that most identified circRNAs are unlikely to encode peptides.

Validation of candidate genes by RT-qPCR

To further validate the *ITGB5*-associated multilayered regulatory landscape suggested by our enrichment and network analyses, we selected three representative DETs for RT-qPCR validation: *DAG1* (mRNA; encoding dystroglycan 1, an ECM receptor), *SNHG1* (lncRNA; a reported oncogenic lncRNA), and *circFN1* (a circRNA derived from the *FN1* gene). These candidates were prioritized because they were integral to our pathway-focused analyses linked to the PI3K/Akt and MAPK/ERK signaling axes. RT-qPCR confirmed that the expression levels of all three transcripts were significantly upregulated in *ITGB5*-overexpressing cells compared with the vector controls [Figure 7A-C], consistent with the RNA-seq results. Detailed results are presented in Supplementary Table 11.

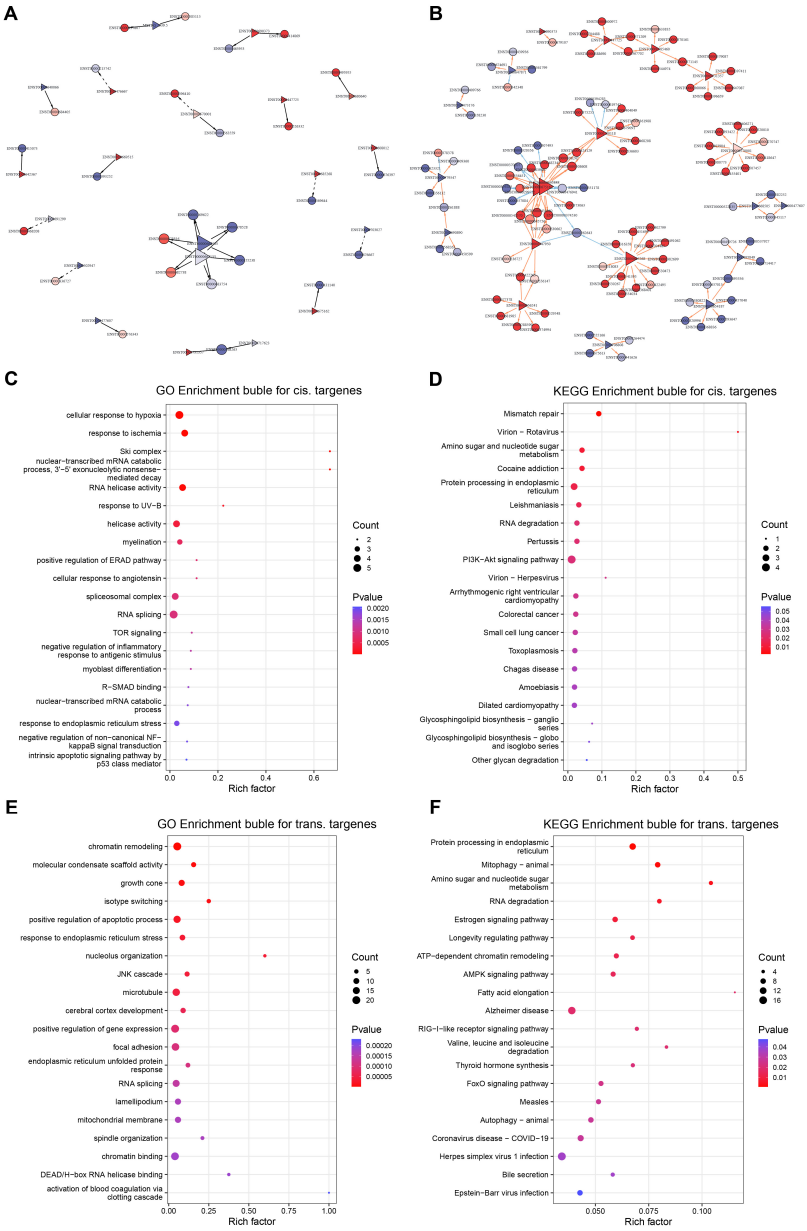


Figure 5. Predicted long non-coding RNAs (lncRNA) targets and functional enrichment profiles. (A) *Cis*-target regulatory network of *ITGB5*-responsive lncRNAs; (B) *Trans*-target regulatory network of *ITGB5*-responsive lncRNAs; (C) GO enrichment bubble plot depicting *cis*-target genes; (D) KEGG enrichment bubble plot depicting *cis*-target genes; (E) GO enrichment bubble plot depicting *trans*-target genes; (F) KEGG enrichment bubble plot depicting *trans*-target genes. DEGs: Differentially expressed genes; DETs: differentially expressed transcripts; GO: gene ontology; KEGG: kyoto encyclopedia of genes and genomes; PI3K/Akt: phosphoinositide 3-kinase/protein kinase B; UV-B: ultraviolet B; ERAD: endoplasmic reticulum-associated degradation; TOR: target of rapamycin; R-SMAD: receptor-regulated SMAD; NF: nuclear factor; JNK: c-Jun N-terminal kinase; ATP: adenosine triphosphate; AMPK: AMP-activated protein kinase; RIG: retinoic acid-inducible gene.

DISCUSSION

HCC remains a leading cause of cancer-related mortality worldwide, with advanced-stage disease exhibiting a particularly poor prognosis due to limited effective therapeutic options[18,19]. The pronounced molecular heterogeneity of HCC continues to impede the development of broadly effective targeted therapies, underscoring the urgent need to elucidate the novel regulatory networks that drive hepatocarcinogenesis[20-22]. In this context, our integrated transcriptomic analyses identify *ITGB5* as a candidate regulatory hub associated with complex coding and non-coding RNA networks. These findings provide a systems-level

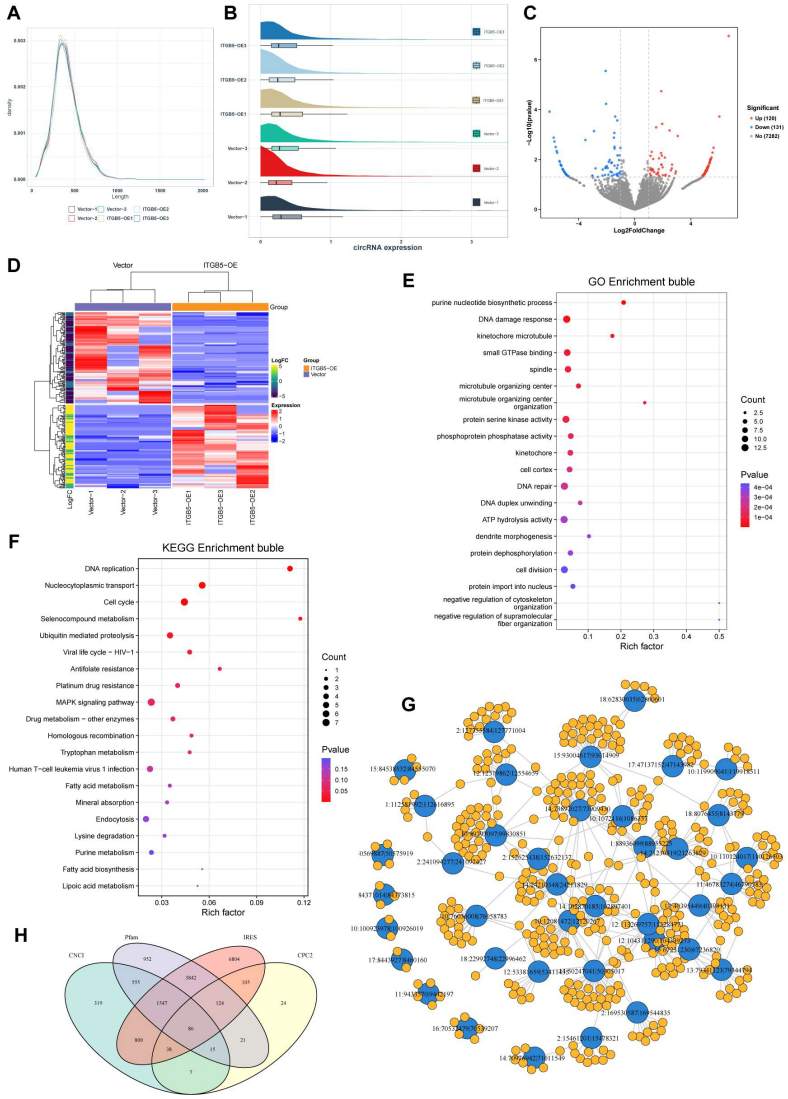


Figure 6. Characterization of circular RNAs (circRNAs) and functional enrichment analysis of their host genes. (A) Length distribution of identified circRNAs; (B) Box plot illustrating the distribution of circRNA expression across samples; (C) Volcano plot depicting differentially expressed circRNAs; (D) Heatmap showing differentially expressed circRNAs with unsupervised hierarchical clustering; (E) GO enrichment bubble plot for the host genes of dysregulated circRNAs; (F) KEGG enrichment bubble plot of the host genes for dysregulated circRNAs; (G) Predicted circRNA-miRNA interaction network; (H) Venn diagram illustrating circRNAs with predicted coding potential based on four algorithms: CNCI, Pfam, IRES, and CPC2. GO: Gene ontology; KEGG: kyoto encyclopedia of genes and genomes; CNCI: coding-non-coding index; IRES: internal ribosome entry site; CPC2: coding potential calculator; ATP: adenosine triphosphate; MAPK: mitogen-activated protein kinase.

perspective on *ITGB5*-driven regulatory mechanisms and their specific roles in HCC pathobiology.

The high mortality associated with HCC is largely attributable to its aggressive clinical behavior and intrinsic resistance to conventional treatments[4,23]. Increasing evidence suggests that dysregulated signaling networks and complex tumor-microenvironment interactions play pivotal roles in driving HCC progression[24,25]. Within this landscape, integrins have emerged as key coordinators of ECM communication, integrating biochemical and mechanical cues to modulate cell adhesion, migration, proliferation, and survival. *ITGB5*, in particular, has been linked to invasive growth and metastatic dissemination across multiple malignancies[9,26]. Despite these advances, the global downstream transcriptomic landscape governed by *ITGB5* in HCC - particularly concerning lncRNAs and circRNAs - remains largely unexplored. Our study addresses this knowledge gap by characterizing *ITGB5*-regulated coding and non-coding RNA networks and

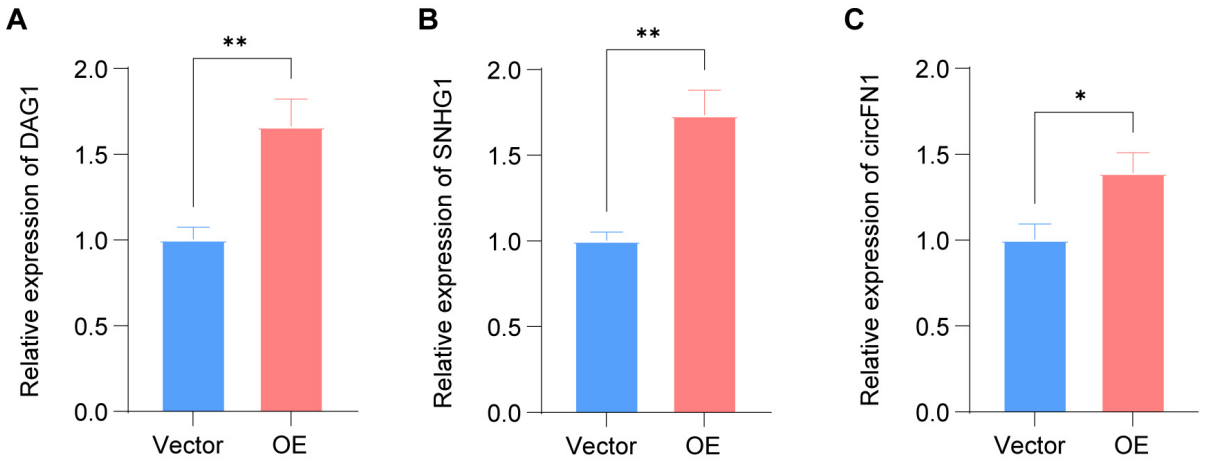


Figure 7. Validation of key regulatory nodes following *ITGB5* overexpression by RT-qPCR. The relative expression levels of three selected candidate molecules were assessed: (A) *DAG1* mRNA, (B) SNHG1 lncRNA, and (C) *circFN1*. Data are presented as mean ± SD (n = 3). Statistical significance was determined using an unpaired two-tailed Student's *t*-test. $^{*}P < 0.05$, $^{**}P < 0.01$. RT-qPCR: Real-time quantitative polymerase chain reaction; mRNA: messenger RNA; lncRNA: long non-coding RNAs; OE: overexpression; SD: standard deviation.

demonstrating their convergence on core oncogenic signaling pathways.

Paradoxically, our observation that PI3K/Akt signaling is consistently suppressed following *ITGB5* overexpression contrasts with the widely recognized role of *ITGB5* in promoting PI3K/Akt activation[27,28]. However, this finding aligns with accumulating evidence that integrin-mediated signaling is governed by intricate, often nonlinear regulatory architectures. Prior studies have demonstrated that integrin engagement can activate a PI3K-ARAP3 (ArfGAP with RhoGAP domain, ankyrin repeat and PH domain 3)-dependent negative feedback loop that locally attenuates PI3K activity[29], offering a plausible mechanistic basis for the suppression observed in our model. Moreover, extensive crosstalk among the FAK/Src, PI3K/Akt, and MAPK pathways has been well documented, and recent reviews emphasize the profound context dependence of integrin signaling and its ability to reprogram downstream outputs under distinct cellular states[30]. Supporting this context specificity, the integrin-PI3K/Akt axis exhibits cell type-dependent signaling patterns in HCC models, including HepG2 cells[31]. Computational systems biology analyses further reinforce this view by demonstrating that relative protein abundance and signaling stoichiometry critically shape pathway prioritization and output specificity[32]. Additionally, the suppression of PI3K/Akt signaling may reflect an adaptive response to oncogenic stress, wherein cancer cells activate compensatory programs, such as stress-response pathways, autophagy, and metabolic rewiring, to maintain cellular homeostasis under persistent oncogenic pressure[33,34]. Together, these literature-based considerations may explain the paradoxical PI3K/Akt suppression observed in our study; however, these mechanisms were not directly tested here and should therefore be interpreted cautiously.

Our data suggest that *ITGB5* is associated with alterations in the expression of both lncRNAs and circRNAs, thereby influencing key cellular processes, including PI3K/Akt signaling, endoplasmic reticulum stress responses, and cell cycle regulation. Notably, *ITGB5* overexpression upregulated *DAG1*, *SNHG1*, and *circFN1* - molecules intimately linked to PI3K/Akt and MAPK/ERK signaling - yet was associated with the suppression of PI3K/Akt signaling and the preferential activation of MAPK/ERK in HepG2 cells. This non-canonical pattern highlights the context-dependent nature of *ITGB5*-mediated signaling and suggests the presence of finely tuned feedback and compensatory mechanisms.

A representative example of this context-dependence is *DAG1*. Although the dystroglycan complex is generally associated with PI3K/Akt activation, our findings indicate that PI3K/Akt signaling is suppressed in *ITGB5*-overexpressing cells despite *DAG1* upregulation. This apparent discrepancy may reflect the functional duality of *DAG1*, which can exert either activating or inhibitory effects depending on the cellular context. In our system, *ITGB5*-associated upregulation of *DAG1* may be linked to context-specific inhibitory effects. Furthermore, the intracellular domain of dystroglycan has been reported to facilitate ERK activation by recruiting MEK/ERK components to the plasma membrane[35], a mechanism that likely contributes to the enhanced MAPK/ERK signaling observed in our HCC model.

Recent studies have highlighted the multifaceted roles of non-coding RNAs, including lncRNAs, circRNAs, and other small RNA species, in oncogenic regulation. In this context, lncRNAs are known to modulate cancer-related biological processes such as migration, invasion, proliferation, and apoptosis, while circRNAs often function as miRNA sponges or protein regulators, thereby contributing to tumor progression through various signaling pathways[36,37]. These observations further support the biological relevance of the lncRNA- and circRNA-associated regulatory landscapes identified in the present study. Among these, SNHG1 has been reported to promote tumorigenesis via ceRNA-mediated sequestration of tumor-suppressive miRNAs, such as miR-195, thereby activating the PI3K/Akt/mechanistic target of rapamycin (mTOR) signaling axis[38-40]. Intriguingly, in *ITGB5*-overexpressing HepG2 cells, *SNHG1* upregulation was accompanied by suppression of the PI3K/Akt pathway and activation of the MAPK/ERK signaling. This finding suggests a potential reprogramming of signaling hierarchies under *ITGB5*-high conditions, although the underlying ceRNA mechanisms remain to be fully elucidated. Given that *ITGB5* predominantly signals through the focal adhesion kinase (FAK)/Src/RAS (rat sarcoma)/ERK cascade, this route may become the dominant signaling output under *ITGB5*-high conditions. Consequently, PI3K/Akt suppression may emerge from robust negative feedback or enhanced phosphatase activity [e.g., phosphatase and tensin homolog (PTEN) or SH2-containing inositol phosphatase (SHIP)][41,42].

Similarly, PI3K/Akt suppression may involve the *circFN1*-miR-182 regulatory axis. Although *circFN1* has been reported to function as a competing ceRNA that sponges miR-182, the downstream effects of miR-182 vary significantly across cancer types[43,44]. In our model, *circFN1*-associated regulation may be linked to PI3K/Akt inhibition, suggesting a context-dependent outcome. Furthermore, *circFN1* has been documented to interact with miR-218, thereby influencing MAPK signaling[45] and potentially contributing to pathway crosstalk Supplementary Figure 4. However, these interactions were not experimentally validated in the present study and warrant further investigation.

Through targeted RT-qPCR validation, we confirmed the dysregulation of representative RNA regulators, including *DAG1*, *SNHG1*, and *circFN1*, thereby supporting the robustness of our transcriptomic findings. The high concordance between our sequencing data and RT-qPCR results strengthens the reliability of the *ITGB5*-associated regulatory network identified in this study.

The translational relevance of our findings is noteworthy. Recent studies have emphasized that integrated biomarker strategies are increasingly pivotal for cancer classification and personalized management[46]. In this context, the *ITGB5*-associated RNA network identified herein may provide a preliminary framework for RNA-based biomarker development and molecular stratification in HCC. In addition, the growing interest in utilizing non-coding RNAs as diagnostic and prognostic tools[47] further supports the clinical relevance of these findings. However, these implications remain preliminary and require rigorous validation in independent clinical cohorts and through further functional studies.

Nonetheless, several limitations of this study should be noted. First, our findings are primarily based on in vitro cellular models, which, although suitable for mechanistic exploration, require further validation in animal models and patient-derived tissues to establish their physiological and clinical relevance. Furthermore, all experiments were conducted exclusively in HepG2 cells. While HepG2 is a widely utilized HCC model, validation in additional cell lines - such as Huh7 or LM3 (human hepatocellular carcinoma cell lines) - is necessary to confirm the broader applicability of our findings. Second, the inferred modulation of key signaling pathways, particularly PI3K/Akt and MAPK/ERK, is based predominantly on transcriptomic data. As RNA-level changes do not necessarily reflect protein abundance or activation status - especially for signaling molecules regulated by phosphorylation - protein-level validation of representative components, such as the phosphorylation status of AKT and ERK, would provide essential complementary evidence. Accordingly, future studies will prioritize such experiments to further substantiate the role of *ITGB* in regulating signaling mechanisms. Third, although we have delineated an *ITGB5*-associated transcriptomic network, the precise regulatory relationships among its components remain to be fully elucidated. Crucially, because *ITGB5* knockdown or knockout experiments were not performed, a direct causal relationship between *ITGB5* and the observed transcriptomic alterations cannot be established. Similarly, while *DAG1*, *SNHG1*, and *circFN1* were identified as *ITGB5*-associated candidates, their direct or indirect regulation by *ITGB5*, as well as the underlying mechanisms - including transcriptional control and potential competing ceRNA interactions - require rigorous experimental validation. Additionally, integrin-mediated signaling is inherently complex and involves extensive crosstalk among different integrin subunits. ITGB5 forms heterodimers with specific α subunits, and alterations in its expression may influence the composition and balance of integrin complexes at the cell surface[48]. Moreover, different integrin complexes can converge on shared signaling nodes, including the FAK/Src, PI3K/Akt, and MAPK/ERK pathways, enabling cooperative or competitive regulation of downstream signaling outputs[49]. In HCC, such network-level interactions are plausible, as other integrin modules have also been linked to AKT/mTOR and FAK-associated signaling[31]. Therefore, the signaling effects observed in this study may be influenced, at least in part, by interactions with other integrin subunits; however, these crosstalk mechanisms were not directly investigated and warrant further evaluation. Finally, the lack of validation in clinical HCC samples represents an additional limitation. Future studies should incorporate clinical specimens to investigate the clinical associations between *ITGB5*, its downstream RNA candidates, and specific clinicopathological features or patient outcomes.

Moving forward, further work is needed to clarify how *ITGB5* regulates *DAG1*, *SNHG1*, and *circFN1* at the transcriptional or post-transcriptional levels, to define their functional roles through gain- and loss-of-function assays, and to determine how these effectors collectively influence the balance between PI3K/Akt and MAPK/ERK signaling. The integration of these regulatory mechanisms within the *ITGB5*-driven oncogenic network remains a key area for future investigation.

Conclusion

In conclusion, our integrated transcriptomic profiling indicates that *ITGB5* overexpression is associated with coordinated alterations of coding and non-coding RNAs in HCC, exemplified by *DAG1*, *SNHG1*, and *circFN1*, and with prominent involvement of the PI3K/Akt and MAPK/ERK signaling axes. These results expand our understanding of *ITGB5*-linked transcriptional reprogramming in HCC and identify *ITGB5* and selected downstream RNA effectors as candidate biomarkers and potential therapeutic targets for further validation in clinically relevant models.

DECLARATIONS

Acknowledgments

The Graphical Abstract was created with BioRender.com and is available at: https://app.biorender.com/illustrations/6980711e720b70dc99a86a98.

Authors' contributions

Made substantial contributions to conception and design of the study: Yang, D.; Chen, X.

Developed the methodology and performed the investigation: Shen, W.; Wang, J.; Zeng, Q.
Performed formal analysis and interpreted the data: Xin, Q.; Lin, Z.; Li, G.
Performed data curation and drafted the original manuscript: Shen, W.
Provided project administration, supervision, and funding acquisition: He, J.; Yang, D.
Revised and edited the manuscript: He, J.; Yang, D.; Chen, X.
All authors read and approved the submitted version.

Availability of data and materials

RT-qPCR source data are provided in the Supplementary Materials. RNA-seq raw data are being prepared for submission to the Sequence Read Archive (SRA) and will be made publicly available upon completion of the deposition process.

AI and AI-assisted tools statement

Not applicable.

Financial support and sponsorship

This work was supported by grants from Noncommunicable Chronic Diseases-National Science and Technology Major Project (2024ZD0531200); National Natural Science Foundation of China (82172205, 82402915, 82302842, 82560451); Guangdong Basic and Applied Basic Research Foundation (2023A1515140123, 2024A1515220094, 2024A1515140053, 2025A1515012214); The Medical Clinical Key Specialty Construction Project for 14th Five-Year Plan of Guangdong Province; The Medical High Level-Key Specialty Construction Project for 14th Five-Year Plan of Foshan City; Foshan Key Laboratory of Tissue Engineering for Skin and Precision Diagnosis and Treatment of Infectious Skin Diseases; National Key Clinical Specialty Construction Program (Department of Burns, Plastic Surgery and Wound Repair).

Conflicts of interest

All authors declared that there are no conflicts of interest.

Ethical approval and consent to participate

Not applicable.

Consent for publication

Not applicable.

Copyright

© The Author(s) 2026.

Supplementary Materials

Supplementary Materials

REFERENCES

1. Bray F, Laversanne M, Sung H, et al. Global cancer statistics 2022: GLOBOCAN estimates of incidence and mortality worldwide for 36 cancers in 185 countries. *CA Cancer J Clin.* 2024;74:229-63. DOI
2. Singal AG, Kanwal F, Llovet JM. Global trends in hepatocellular carcinoma epidemiology: implications for screening, prevention and therapy. *Nat Rev Clin Oncol.* 2023;20:864-84. DOI
3. Luo Y, Zhu H. Immunotherapy for advanced or recurrent hepatocellular carcinoma. *World J Gastrointest Oncol.* 2023;15:405-24. DOI PubMed PMC
4. Zou Y, Wan X, Zhou Q, et al. Mechanisms of drug resistance in hepatocellular carcinoma. *Biol Proced Online.* 2025;27:19. DOI PubMed PMC
5. Lee YR. A multidisciplinary approach with immunotherapies for advanced hepatocellular carcinoma. *J Liver Cancer.* 2023;23:316-29. DOI PubMed PMC
6. Yuan Z, Yan K, Wang J. Overexpression of integrin β2 improves migration and engraftment of adipose-derived stem cells and augments angiogenesis in myocardial infarction. *Ann Transl Med.* 2022;10:863. DOI PubMed PMC

7. Zhang L, Guo Q, Guan G, Cheng W, Cheng P, Wu A. Integrin beta 5 is a prognostic biomarker and potential therapeutic target in glioblastoma. *Front. Oncol.* 2019;9:904. DOI PubMed PMC
8. Shi W, He J, Huang Y, et al. Integrin β5 enhances the malignancy of human colorectal cancer by increasing the TGF-β signaling. *Anticancer Drugs.* 2021;32:717-26. DOI
9. Cheng Y, Lin X, Xu H, et al. Integrin β5, a noninvasive diagnostic biomarker, is associated with unfavorable prognosis and immunotherapy efficacy in gastric cancer. *BMC Gastroenterol.* 2024;24:362. DOI PubMed PMC
10. Chen Z, Fang Y, Zhong S, Lin S, Yang X, Chen S. ITGB5 is a prognostic factor in colorectal cancer and promotes cancer progression and metastasis through the Wnt signaling pathway. *Sci Rep.* 2025;15:9225. DOI PubMed PMC
11. Lin Z, He R, Luo H, et al. RETRACTED ARTICLE: integrin-β5, a miR-185-targeted gene, promotes hepatocellular carcinoma tumorigenesis by regulating β-catenin stability. *J Exp Clin Cancer Res.* 2018;37:17. DOI PubMed PMC
12. Shi Y, Wang J, Huang G, et al. A novel epithelial-mesenchymal transition gene signature for the immune status and prognosis of hepatocellular carcinoma. *Hepatol Int.* 2022;16:906-17. DOI
13. Shang L, Ye X, Zhu G, et al. Prognostic value of integrin variants and expression in post-operative patients with HBV-related hepatocellular carcinoma. *Oncotarget.* 2017;8:76816-31. DOI PubMed PMC
14. Yang X, Qin C, Zhao B, et al. Long noncoding RNA and circular RNA: two rising stars in regulating epithelial-mesenchymal transition of pancreatic cancer. *Front. Oncol.* 2022;12:910678. DOI PubMed PMC
15. Ma Q, Yang F, Xiao B, Guo X. Emerging roles of circular RNAs in tumorigenesis, progression, and treatment of gastric cancer. *J Transl Med.* 2024;22:207. DOI PubMed PMC
16. Bao Z, Yang Z, Huang Z, Zhou Y, Cui Q, Dong D. LncRNADisease 2.0: an updated database of long non-coding RNA-associated diseases. *Nucleic Acids Res.* 2019;47:D1034-7. DOI PubMed PMC
17. Kopp F, Mendell JT. Functional classification and experimental dissection of long noncoding RNAs. *Cell.* 2018;172:393-407. DOI PubMed PMC
18. Hwang SY, Danpanichkul P, Agopian V, et al. Hepatocellular carcinoma: updates on epidemiology, surveillance, diagnosis and treatment. *Clin Mol Hepatol.* 2025;31 Suppl:S228-54. DOI PubMed PMC
19. Li K, Mathew B, Saldanha E, et al. New insights into biomarkers and risk stratification to predict hepatocellular cancer. *Mol Med.* 2025;31:152. DOI PubMed PMC
20. Zhai W, Lai H, Kaya NA, et al. Dynamic phenotypic heterogeneity and the evolution of multiple RNA subtypes in hepatocellular carcinoma: the PLANET study. *Natl Sci Rev.* 2022;9:nwab192. DOI PubMed PMC
21. Zhu S, Hoshida Y. Molecular heterogeneity in hepatocellular carcinoma. *Hepat. Oncol.* 2018;5:HEP10. DOI PubMed PMC
22. Chen S, Cao Q, Wen W, Wang H. Targeted therapy for hepatocellular carcinoma: challenges and opportunities. *Cancer Lett.* 2019;460:1-9. DOI
23. Likhitsup A, Razumilava N, Parikh ND. Treatment for advanced hepatocellular carcinoma: current standard and the future. *Clin Liver Dis.* 2019;13:13-9. DOI PubMed PMC
24. Liu P, Kong L, Liu Y, Li G, Xie J, Lu X. A key driver to promote HCC: cellular crosstalk in tumor microenvironment. *Front. Oncol.* 2023;13:1135122. DOI PubMed PMC
25. Farzaneh Z, Vosough M, Agarwal T, Farzaneh M. Critical signaling pathways governing hepatocellular carcinoma behavior; small molecule-based approaches. *Cancer Cell Int.* 2021;21:208. DOI PubMed PMC
26. Huang L, Lu Y, He R, et al. N4-acetylcytidine modification of ITGB5 mRNA mediated by NAT10 promotes perineural invasion in pancreatic ductal adenocarcinoma. *J Exp Clin Cancer Res.* 2025;44:103. DOI PubMed PMC
27. Wen X, Chen S, Chen X, et al. ITGB5 promotes innate radiation resistance in pancreatic adenocarcinoma by promoting DNA damage repair and the MEK/ERK signaling pathway. *Front. Oncol.* 2022;12:887068. DOI PubMed PMC
28. Liu D, Cao J, Hu K, Peng Z. Integrin β5 interacts with G3BP1 through activating FAK/Src signaling pathway to promote gastric carcinogenesis. *Sci Rep.* 2025;15:28633. DOI PubMed PMC
29. Mccormick B, Craig HE, Chu JY, et al. A negative feedback loop regulates integrin inactivation and promotes neutrophil recruitment to inflammatory sites. *J Immunol.* 2019;203:1579-88. DOI PubMed PMC
30. Cooper J, Giancotti FG. Integrin signaling in cancer: mechanotransduction, stemness, epithelial plasticity, and therapeutic resistance. *Cancer Cell.* 2019;35:347-67. DOI PubMed PMC
31. Juratli MA, Zhou H, Oppermann E, et al. Integrin α2 and β1 cross-communication with mTOR/AKT and the CDK-cyclin axis in hepatocellular carcinoma cells. *Cancers.* 2022;14:2430. DOI PubMed PMC
32. Jafarnejad M, Sové RJ, Danilova L, et al. Mechanistically detailed systems biology modeling of the HGF/Met pathway in hepatocellular carcinoma. *npj Syst Biol Appl.* 2019;5:29. DOI PubMed PMC
33. Iovanna J, Estaras M, Grasso D, Fernández Zapico ME, Neira JL, Santofimia-castaño P. Oncogenic stress response mechanisms as new therapeutic targets in cancer treatment: A review. *Medicine.* 2025;104:e42857. DOI

34. Qiu B, Simon MC. Oncogenes strike a balance between cellular growth and homeostasis. *Semin Cell Dev Biol.* 2015;43:3-10. DOI PubMed PMC
35. Spence HJ, Dhillon AS, James M, Winder SJ. Dystroglycan, a scaffold for the ERK-MAP kinase cascade. *EMBO Rep.* 2004;5:484-9. DOI
36. Quan J, Wan Z, Wu W, et al. Classical biomarkers and non-coding RNAs associated with diagnosis and treatment in gastric cancer. *Oncol Res.* 2025;33:1069-89. DOI PubMed PMC
37. Deng X, Liao T, Xie J, et al. The burgeoning importance of PIWI-interacting RNAs in cancer progression. *Sci. China Life Sci.* 2023;67:653-62. DOI
38. Xu S, He L, Chen Y, et al. Clinical implications of miR-195 in cancer: mechanisms, potential applications, and therapeutic strategies. *J Cancer Res Clin Oncol.* 2025;151:148. DOI PubMed PMC
39. Chen J, Wang F, Xu H, et al. Long non-coding RNA SNHG1 regulates the Wnt/β-catenin and PI3K/AKT/mTOR signaling pathways via EZH2 to affect the proliferation, apoptosis, and autophagy of prostate cancer cell. *Front. Oncol.* 2020;10:552907. DOI PubMed PMC
40. Zeng H, Zhou S, Cai W, Kang M, Zhang P. LncRNA SNHG1: role in tumorigenesis of multiple human cancers. *Cancer Cell Int.* 2023;23:198. DOI PubMed PMC
41. Lu Y, Yu Q, Liu JH, et al. Src family protein-tyrosine kinases alter the function of PTEN to regulate phosphatidylinositol 3-kinase/AKT cascades. *J Biol Chem.* 2003;278:40057-66. DOI
42. Azzi A. SHIP2 inhibition alters redox-induced PI3K/AKT and MAP kinase pathways via PTEN over-activation in cervical cancer cells. *FEBS Open Bio.* 2020;10:2191-205. DOI PubMed PMC
43. Huang XX, Zhang Q, Hu H, et al. A novel circular RNA circFN1 enhances cisplatin resistance in gastric cancer via sponging miR-182-5p. *J Cell Biochem.* 2020;122:1009-20. DOI
44. Sameti P, Tohidast M, Amini M, Bahojb Mahdavi SZ, Najafi S, Mokhtarzadeh A. The emerging role of MicroRNA-182 in tumorigenesis; a promising therapeutic target. *Cancer Cell Int.* 2023;23:134. DOI PubMed PMC
45. Wischmann F, Troschel FM, Frankenberg M, et al. Tumor suppressor miR-218 directly targets epidermal growth factor receptor (EGFR) expression in triple-negative breast cancer, sensitizing cells to irradiation. *J Cancer Res Clin Oncol.* 2023;149:8455-65. DOI PubMed PMC
46. Passaro A, Al Bakir M, Hamilton EG, et al. Cancer biomarkers: emerging trends and clinical implications for personalized treatment. *Cell.* 2024;187:1617-35. DOI PubMed PMC
47. Piergentili R, Gullo G, Basile G, et al. Circulating miRNAs as a tool for early diagnosis of endometrial cancer-implications for the fertility-sparing process: clinical, biological, and legal aspects. *Int J Mol Sci.* 2023;24:11356. DOI
48. Samaržija I, Dekanić A, Humphries JD, et al. Integrin crosstalk contributes to the complexity of signalling and unpredictable cancer cell fates. *Cancers.* 2020;12:1910. DOI PubMed PMC
49. Li S, Sampson C, Liu C, Piao H, Liu H. Integrin signaling in cancer: bidirectional mechanisms and therapeutic opportunities. *Cell Commun Signal.* 2023;21:266. DOI PubMed PMC

Disclaimer/Publisher's Note: All statements, opinions, and data contained in this publication are solely those of the individual author(s) and contributor(s) and do not necessarily reflect those of OAE and/or the editor(s). OAE and/or the editor(s) disclaim any responsibility for harm to persons or property resulting from the use of any ideas, methods, instructions, or products mentioned in the content.



© The Author(s) 2026. Open Access This article is licensed under a Creative Commons Attribution 4.0 International License (https://creativecommons.org/licenses/by/4.0/), which permits unrestricted use, sharing, adaptation, distribution and reproduction in any medium or format, for any purpose, even commercially, as long as you give appropriate credit to the original author(s) and the source, provide a link to the Creative Commons license, and indicate if changes were made.